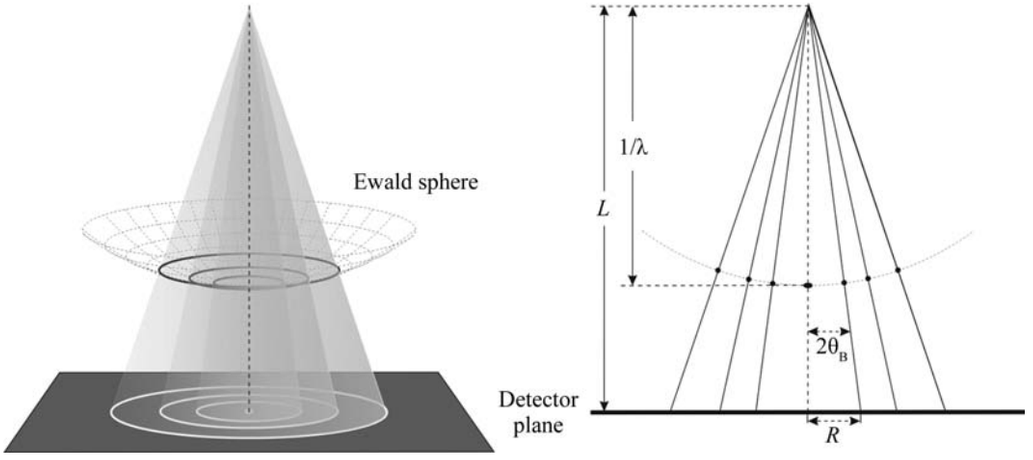


**Figure 2.4.2**
Schematic diagram of the Ewald sphere construction and the geometry for recording electron diffraction patterns.

development in time-resolved electron diffraction at a time resolution approaching femtoseconds (Elsayedali & Herman, 1990; Siwick *et al.*, 2003) will significantly improve the ability to interrogate structures at high spatial and time resolution.

Irradiation of both organic and inorganic materials with an electron beam can cause severe modification of the structure. The amount of energy deposited into the material can be estimated through the ratio of the elastic and inelastic scattering cross sections. For carbon the ratio for electrons (300 keV) and X-rays (with a wavelength of less than 1 Å) is comparable, meaning that the radiation damage caused by these sources is on the same scale (Henderson, 1995). Electron radiation damage is caused by all kinds of ionization processes, including bond breakdown and subsequent recombination of radicals and active molecular species. Inorganic materials can show knock-on damage (atomic displacement) or sputtering effects (loss of atoms). This damage may lead to a total structural collapse. The collective damage due to electron radiation is quantified using the electron dose and electron dose rates. In many cases the damage can be reduced by minimizing the electron dose received by the sample, cryo-protection, or deposition of a protective conductive layer (Reimer & Kohl, 2008).

This chapter covers the practical issues and theory of electron powder diffraction as well as applications for material analysis. A fundamental description of electron diffraction can be found in *International Tables for Crystallography*, Vol. C (2004) and the book by Zuo & Spence (2017). The present chapter is subdivided into seven sections. Sections 2.4.2 and 2.4.3 cover the theory and the experimental setup of an electron powder diffraction experiment using transmission electron microscopes, respectively. Sections 2.4.4 and 2.4.5 discuss the application of electron powder diffraction data to phase and texture analysis and related techniques. Rietveld refinement with electron powder diffraction data is a relatively new field; this is discussed in Section 2.4.6. The last section reviews pair distribution function (PDF) analysis using electron diffraction data.

### 2.4.2. Electron powder diffraction pattern geometry and intensity

By J.-M. Zuo and J. L. Lábár

The powder diffraction rings in transmission geometry appear where the cone of diffracted electron beams intersects the Ewald sphere. The intersection creates a ring of diffracted beams, which is then projected onto the planar detector (see Fig. 2.4.2) with a radius ($R$) according to

$$R = L \tan 2\theta_{\rm B}. \tag{2.4.1}$$

Here $\theta_{\rm B}$ is the Bragg diffraction angle and $L$ is the camera length.

The $d$-spacing can be obtained by measuring the length of $R$ in an experimental diffraction pattern using

$$d = \frac{\lambda}{2 \sin \theta_{\rm B}}. \tag{2.4.2}$$

The electron wavelength is determined by the electron accelerating voltage ($\Phi$), in volts:

$$\lambda = \frac{h}{(2m_e\Phi)^{1/2}} \simeq \frac{1.226}{[\Phi(1 + 0.97845 \times 10^{-6}\Phi)]^{1/2}}. \tag{2.4.3}$$

The wavelength of high-energy electrons is relatively short. For 200 kV electrons, the wavelength is 0.025 Å and the Bragg angle is very small. For example, for $d$ = 2.5 Å the electron scattering angle $\theta$ is 5 mrad. For a small Bragg angle one can use the approximation $\sin\theta \simeq \tan\theta \simeq \theta$. This gives the relationship

$$d \simeq \frac{L\lambda}{Rd}. \tag{2.4.4}$$

At large scattering angles with $\sin\theta/\lambda$ 2 Å$^{-1}$ or greater, a better approximation is given by (Cowley & Hewat, 2004)

$$d \simeq \frac{L\lambda}{R}\left(1 + \frac{3R^2}{8L^2}\right). \tag{2.4.5}$$

The camera length $L$ can be determined using a sample with known $d$-spacings, while the electron wavelength or acceleration voltage can be calibrated using high-order Laue zone (HOLZ) lines in convergent-beam electron diffraction (CBED) patterns (Zuo, 1993).

For a small parallelepiped crystal fully illuminated by a coherent electron beam of intensity $I_0$, the kinematic diffraction intensity is given by

$$I_{\rm SC} = I_0 \frac{\left|F_{hkl}\right|^2}{L^2} \left\{\frac{\sin[\pi \mathbf{S}_{hkl} \cdot N_1\mathbf{a}]}{\sin[\pi \mathbf{S}_{hkl} \cdot \mathbf{a}]} \frac{\sin[\pi \mathbf{S}_{hkl} \cdot N_2\mathbf{b}]}{\sin[\pi \mathbf{S}_{hkl} \cdot \mathbf{b}]} \frac{\sin[\pi \mathbf{S}_{hkl} \cdot N_3\mathbf{c}]}{\sin[\pi \mathbf{S}_{hkl} \cdot \mathbf{c}]}\right\}^2, \tag{2.4.6}$$

where $N_1$, $N_2$ and $N_3$ are the number of unit cells along the three axis directions, and $F_{hkl}$ is the electron structure factor of the $hkl$ reflection: